



Ocular wavefront aberrations in the common marmoset *Callithrix jacchus*: Effects of age and refractive error

Nancy J. Coletta^{a,*}, Susana Marcos^b, David Troilo^c

^aThe New England College of Optometry, Boston, MA, United States

^bInstituto de Optica, Consejo Superior de Investigaciones Cientificas, Madrid, Spain

^cState University of New York, College of Optometry, New York, NY, United States

ARTICLE INFO

Article history:

Received 1 February 2010

Received in revised form 19 August 2010

Keywords:

Optical aberrations

Development

Emmetropization

Refractive error

Marmoset

Primate

ABSTRACT

The common marmoset, *Callithrix jacchus*, is a primate model for emmetropization studies. The refractive development of the marmoset eye depends on visual experience, so knowledge of the optical quality of the eye is valuable. We report on the wavefront aberrations of the marmoset eye, measured with a clinical Hartmann–Shack aberrometer (COAS, AMO Wavefront Sciences). Aberrations were measured on both eyes of 23 marmosets whose ages ranged from 18 to 452 days. Twenty-one of the subjects were members of studies of emmetropization and accommodation, and two were untreated normal subjects. Eleven of the 21 experimental subjects had worn monocular diffusers and 10 had worn binocular spectacle lenses of equal power. Monocular deprivation or lens rearing began at about 45 days of age and ended at about 108 days of age. All refractions and aberration measures were performed while the eyes were cycloplegic; most aberration measures were made while subjects were awake, but some control measurements were performed under anesthesia. Wavefront error was expressed as a seventh-order Zernike polynomial expansion, using the Optical Society of America's naming convention. Aberrations in young marmosets decreased up to about 100 days of age, after which the higher-order RMS aberration leveled off to about 0.10 μm over a 3 mm diameter pupil. Higher-order aberrations were 1.8 times greater when the subjects were under general anesthesia than when they were awake. Young marmoset eyes were characterized by negative spherical aberration. Form-deprived eyes of the monocular deprivation animals had greater wavefront aberrations than their fellow untreated eyes, particularly for asymmetric aberrations in the odd-numbered Zernike orders. Both lens-treated and form-deprived eyes showed similar significant increases in Z_3^{-3} trefoil aberration, suggesting the increase in trefoil may be related to factors that do not involve visual feedback.

© 2010 Elsevier Ltd. All rights reserved.

1. Introduction

In the study of refractive development, animal models allow one to perform longitudinal studies and manipulations of visual experience that would be difficult or impossible to accomplish in humans. Form deprivation or lens-rearing alter the emmetropization process in a number of species, particularly when applied during development (Howlett & McFadden, 2006; Hung, Crawford, & Smith, 1995; Lu et al., 2006; Norton, 1990; Norton & McBrien, 1992; Schaeffel, Burkhardt, Howland, & Williams, 2004; Smith, Bradley, Fernandes, & Boothe, 1999; Smith, Hung, & Harwerth, 1994; Troilo & Judge, 1993; Troilo, Li, Glasser, & Howland, 1995; Troilo & Nickla, 2005; Troilo, Nickla, & Wildsoet, 2000a, 2000b; Troilo, Totonelly, & Harb, 2009; Troilo & Wallman, 1991; Wallman

& Winawer, 2004; Wallman et al., 1995; Whatham & Judge, 2001; Wildsoet, 1997; Wildsoet & Wallman, 1995; Zhou et al., 2008). Generally, a degradation of retinal image quality or exposure to hyperopic defocus results in myopia. As the time-scale of development is much shorter in these species than it is in humans, it is possible to monitor changes in ocular biometry and geometry, such as the anterior and posterior chamber depth, lens thickness, and keratometry, during the development of refractive errors, in comparison with the normal emmetropization of the eye. The induction of myopia generally results from an excessive axial length.

It is well accepted that proper emmetropization requires visual feedback, as the drastic reduction of contrast and spatial frequency induced by diffusers generally results in myopia (Diether, Gekeler, & Schaeffel, 2001). However, it has not been until recently that the quality of the natural optics has been studied in the widely used animal myopia models. The optical quality of the chick eye, both untreated and after form deprivation myopia, was first measured using a double-pass technique (Coletta, Marcos, Wildsoet, & Troilo,

* Corresponding author. Address: 424 Beacon Street, Boston, MA 02115, United States.

E-mail address: colettan@neco.edu (N.J. Coletta).

2003). More recently, Hartmann–Shack aberrometry has been used to measure the aberrations of developing normal and myopic chick eyes (Garcia de la Cera, Rodriguez, & Marcos, 2006a; Garcia de la Cera, Rodriguez, de Castro, Merayo, & Marcos, 2007; Ksilak, Campbell, Hunter, Irving, & Huang, 2006; Tian & Wildsoet, 2006). Although there are differences across studies, most likely associated with the different treatments of optical diffusers and negative-lens rearing, it is well accepted that the optical quality of the adult chicken eye is nearly diffraction-limited. For a constant pupil size, the optical aberrations decrease during development. Eyes with myopia that resulted from treatment also showed a tendency for improvement during development, although they showed greater higher-order aberrations than their contralateral untreated eyes (Garcia de la Cera et al., 2006a). The results suggest that increased aberrations in myopic eyes are caused by axial elongation and are likely to be the result, rather than the cause, for myopia development. The mouse is an emerging model for myopia, but, in contrast to the high quality of chick eyes, mouse eyes have poor optical quality with relatively high amounts of higher-order aberrations (Garcia de la Cera, Rodriguez, Llorente, Schaeffel, & Marcos, 2006b). Treatments intended to induce myopia are challenged by the large depth-of-focus produced by the low quality optics in the mouse eye (Schaeffel et al., 2004; Tejedor & de la Villa, 2003).

Primate models of myopia have been developed in an attempt to reproduce the structural and optical development of human eyes. Rhesus monkeys have been shown to respond to optically induced defocus and to form deprivation by altering their growth pattern, when the treatment is performed during infancy or adolescence (Smith et al., 1994, 1999). A recent report of the high order ocular aberrations in Rhesus monkeys show a clear decrease in their magnitude during development; by adolescence at around 4 years of age, the optical quality is practically diffraction-limited and the 3rd–5th order Zernike terms are not significantly different from zero (Ramamirtham et al., 2007). Emmetropic Rhesus monkey eyes, following form deprivation or lens-rearing, showed higher amounts of aberrations than emmetropic eyes in both total RMS, coma, spherical aberration and trefoil (Ramamirtham et al., 2007). Interestingly, eyes that recovered from the experimentally induced refractive errors, following a period of unrestricted vision, also showed a decrease in the amounts of higher-order aberrations. In general, the amount of aberrations was correlated with the amount of ametropia. As had previously been observed in chicks, both emmetropic and ametropic Rhesus monkey eyes experience a reduction of higher-order aberration with development.

Another suitable primate experimental myopia model is the common marmoset, *Callithrix jacchus* (Troilo & Judge, 1993). It is easily bred in captivity, the adult ocular dimensions are at a 1:2 scale compared to the human eye, and it reaches adolescence by 200 days of age, a shorter period than macaques (Graham & Judge, 1999). Lid-suture form deprivation and optical diffusers induce refractive errors when the treatment is performed shortly after birth, or at later ages during development (Troilo & Nickla, 2005). Degradation of retinal image quality by diffusers generally produces myopia in marmosets, although the response is variable and a percentage of eyes either do not respond to treatment or develop hyperopia (Troilo & Nickla, 2005). Rearing marmosets with negative contact lenses produces axial elongation and myopia, while rearing with positive contact lenses reduces eye growth and results in hyperopia (Troilo et al., 2009; Whatham & Judge, 2001). The change in eye growth and refractive state in response to spectacle lens rearing in marmosets has been shown, however, to be less well correlated with the power of the treating lens (Troilo & Nickla, 2000; Troilo, Quinn, & Baker, 2007).

The changes of ocular biometry and keratometry of the marmoset eye have been well characterized as a function of aging and refractive error. However, the ocular aberrations of the marmoset

eye have not been reported, except for meeting abstracts presented by our group using either a double-pass technique or Hartmann–Shack aberrometry (Coletta, Troilo, & Marcos, 2001; Coletta, Troilo, Moskowitz, Nickla, & Marcos, 2003, 2004). In this study, ocular aberrations of the infant and adolescent marmoset will be presented for normal and ametropic eyes, as in previous studies that describe ocular aberrations in chickens (Garcia de la Cera et al., 2006a, 2007; Ksilak et al., 2006), Rhesus monkeys (Ramamirtham et al., 2007) and tree-shrews (Ramamirtham, Norton, Siegart, & Roorda, 2003). The results will give insights on the relationships between optical biometry and aberrations, on the emmetropization of aberrations, and on the potential cause-effect relationships between aberrations and ametropia. These experimental data will also be valuable in current efforts to model the change of aberrations with age and refractive error across species, either by the use of scaled growth (Howland, 2005; Howland, Merola, & Basarab, 2004; Hunter, Campbell, Ksilak, & Irving, 2009) or computer eye models (Garcia de la Cera, 2008). Ultimately, the longitudinal measurements undertaken in these animal models will allow better understanding of the optical changes accompanying ametropia in humans, to date primarily evaluated only through cross-sectional studies.

2. Methods

2.1. Subjects

Measurements were made on both eyes of 23 marmosets that had been reared in a colony at the New England College of Optometry. The subjects' ages ranged from 18 to 452 days. Twenty-one animals were members of other studies of emmetropization and accommodation (Troilo et al., 2007) and two were untreated normal subjects. Eleven of the 21 experimental subjects had worn monocular diffusers over their right eyes, and 10 had worn binocular spectacle lenses of equal power in both eyes. The monocular diffusers, also referred to as occluders, were white translucent hemispheres that covered the entire visual field. Of the 10 lens-treated subjects, one subject had worn +5 D lenses, one subject had worn –3 D lenses, two subjects had worn –5 D lenses and six subjects had worn –7 D lenses. Monocular deprivation or lens rearing began at about 45 days of age and ended at about 108 days of age. Data were available on the two untreated animals only during the age range from 18 to 51 days. Aberration measurements were made in multiple sessions on 11 animals (three monocular deprivation, six lens-treated and two normals subjects) and six of the experimental animals were tested before treatment. All refractions and aberration measures were performed while the eyes were cyclopleged with two drops of 1% cyclopentolate, spaced 5 min apart. Aberration measurements began 30 min after the second drop instillation, while the animals were awake. Keratometry was performed after the COAS measures; the animals were then anesthetized with Saffan (0.2 ml/100 g; Schering-Plough Animal Health, UK), and retinoscopy, Hartinger refractions, and ultrasound biometry were completed within 2 h of the initial cycloplegic drop instillation. Adequate measures were taken to minimize pain or discomfort; all procedures were approved by the Institutional Animal Care and Use Committee of the New England College of Optometry.

2.2. Wavefront aberration measurements

Wavefront aberrations were measured with a COAS (AMO Wavefront Sciences) high-resolution infrared Hartmann–Shack (HS) aberrometer. Wavefront error was expressed as a seventh-order Zernike polynomial expansion, using the Optical Society of America's VSIA taskforce naming convention (Thibos, Applegate, Schwiegerling, & Webb, 2000). Wavefront error was typically calculated

over a 3-mm diameter pupil, about the size of the dilated pupil in the youngest marmosets. The microlens array sampled the pupil every 210 μm , so a 3-mm pupil diameter would be sampled by about 165 lenslets. The equipment was calibrated for second-order aberrations using trial lenses and a spherically-surfaced artificial eye that had a known spherical refractive error of -5.00 D at a 12 mm vertex distance. The mean and standard error of 10 COAS measurements of the artificial eye's spherical refraction at the same vertex distance were -5.10 ± 0.015 D when using only the 2nd order Zernike terms and -5.02 ± 0.020 D when adding the Seidel sphere, calculated from the 4.0 Zernike coefficient (Salmon, West, Gasser, & Kenmore, 2003). The mean and standard error of 10 measures of the 4.0 coefficient of the artificial eye were $+0.0235 \pm 0.0026$ μm for a 6 mm diameter pupil. Trial lenses of various powers were added in front of the artificial eye. Over the range of refractions from -5.00 D to $+5.00$ D, the linear regression of the measured refraction (y) vs. expected refraction (x) was $y = 1.0096x - 0.046$ ($R^2 = 1$) when using only the 2nd order terms, and $y = 1.0023x - 0.0214$ ($R^2 = 1$) when adding the Seidel sphere. When a 2.00 D cylindrical trial lens was added before the eye, the mean measured cylinder power and standard error was 1.97 D \pm 0.017 D.

Wavefront aberrations were examined while the subjects were awake, with the animals being able to blink normally, in order to more accurately reflect the aberrations of the marmoset eye under natural viewing conditions. During measurements, the animal's body was wrapped in a cloth towel and an experimenter held the animal's head near the aberrometer, using the chin rest bar as a support, so that the eye under study could be monitored by the instrument's live video image. Another experimenter used the video image to align the COAS with the eye and to focus the instrument at the eye's pupil plane. Wavefront measurements were taken whenever the eye appeared aligned and the first Purkinje image was in focus. COAS images were generally taken shortly after blinks, within 5–10 s, while the eye was continually monitored with the video image. Measurements were completed during a period of about 5 min for each eye. About 15 images were captured per eye, and of these, generally five images were selected to be analyzed. Among the total of 96 measurement sessions on all eyes, we were able to select 5 images for analysis in 78 of the sessions. For the remaining 18 measurement sessions, 12 eyes had 4 images, 5 eyes had 3 images and only one eye had 2 images selected. Image selection was based on consistency of the COAS refractions and complete, focused appearance of the Hartmann–Shack spot patterns. Images were selected for analysis in which the pupil margin in the spot pattern was circular and unobstructed by the eyelid; we avoided using images with elliptical pupil margins that may have been taken during peripheral fixation. The pupil sizes were relatively stable during the COAS measures on a given eye, indicating that the dilation from the cyclopentolate was effective during the aberration measurements. Across the 78 measurement sessions for which there were five selected images, the relative standard deviation (RSD, or $100 * \text{s.d./mean}$) of the pupil diameter across the images per eye ranged from 0.68% to 7.67%, with an average RSD of 2.27%.

We also measured aberrations on seven marmosets (14 eyes) while they were under general anesthesia (Saffan). For measurements performed with the animal under anesthesia, the animal was placed on a platform attached to the aberrometer's chin rest bar; the animal's head position was adjusted via a separate head rest attached to the instrument table. The live video image was used to align the eye. Wavefront measurements were performed with lid retractors; we took several images within about 1 min and then removed the retractor to restore tear film quality.

The Zernike coefficients derived from each of the selected images for an eye were averaged to determine that eye's wavefront aberration. The RMS wavefront error for third-order through seventh-order terms was used as an overall estimate of higher-order

aberration (HOA). This metric excludes the contribution from piston, tilt, defocus and astigmatism. Zernike coefficients were imported to Matlab (Mathworks) to reconstruct wavefront error maps. The sphere and cylinder power of the eye's refraction were also obtained from the Zernike coefficients, using the 2nd order Zernike terms and power vector (M, J_{45}, J_{180}) analysis (Charman & Jennings, 1976; Salmon et al., 2003). The aberrometer uses infrared light of wavelength of 840 nm, but its software adjusts the refraction for a wavelength of 550 nm by adding -0.71 D to the spherical refraction. This amount is based on the chromatic aberration of an adult human eye (Charman & Jennings, 1976).

We examined the variability of refractions and aberrations across the selected images for each eye in order to assess both the consistency of the ocular alignment and the stability of the accommodative state during measurements. The typical standard deviation for repeated measurements of RMS higher-order aberration in an eye was 0.033 μm for a 3 mm pupil; compared to the overall mean HOA RMS from all eyes and measurement sessions, this is a relative standard deviation of about 20%. The standard deviations of repeated measurements in an eye ranged from 0.035 μm for 3rd order aberration to 0.006 μm for 7th order. If eye alignment were a major source of variability in the repeated measurements, one would expect that asymmetric aberration would exhibit more variability than symmetric aberration. However the repeated measures of 3rd and 4th order aberrations had similar relative standard deviations of 27.6% and 24.3%, respectively. The repeated measures of cylindrical refraction power from each eye had a standard deviation of 0.25 D, on average. This also suggests that ocular alignment in the selected COAS images was fairly stable since astigmatism in the human eye increases with increasing eccentricity of fixation (e.g., Atchison, Pritchard, & Schmid, 2006). To assess the stability of the accommodative state during measurements, we used methods described in Salmon et al. (2003) to estimate repeatability of the COAS refraction readings. This involved computing a power deviation vector for each of the readings per eye, using the differences of each power vector component (M, J_{45}, J_{180}) in a reading from their respective means for that eye. The magnitudes of each eye's deviation vectors were then averaged and squared, and the overall RMS deviation across eyes was taken as the sum of these squares divided by the number of measurement sets. For the 2nd order COAS refractions and a 3 mm pupil, the RMS deviation was 0.3 D, across all eyes and sessions. Refractions tended to be more variable for younger marmosets; the RMS deviation for 29 measurement sets on the animals older than 120 days was 0.13 D which is comparable to the repeatability of the COAS and an autorefractor on the manifest refraction in human subjects (Salmon et al., 2003).

2.3. Biometry and refractions

Corneal curvature, refractions and axial dimensions of the eyes were measured on most days on which the aberrations were measured. Corneal curvature was measured with a hand-held infrared (IR) video keratometer (Schaeffel & Howland, 1987) on 16 of the marmosets while they were awake, just after the COAS measurements. The spherical equivalent refraction was also measured by both retinoscopy and with a Hartinger coincidence refractometer on both eyes of 16 animals during 64 of the sessions in which the COAS aberrations were measured. The Hartinger refractometer had been modified with a supplemental positive lens so that the target beams would easily fit within a 3 mm diameter pupil when the instrument was focused. The modified instrument was re-calibrated using an artificial eye. These white-light refractions were performed after the keratometry, while the animals were under general anesthesia (Saffan). The mean of the retinoscopy and Hartinger coincidence refractometer measurements has been used as

the standard value of refractive state in the marmoset studies from this laboratory (e.g. Troilo & Nickla, 2005). Mean refractions obtained by these two methods ranged from -3.98 D to $+9.82$ D over the group. Ultrasound biometry was also performed after all refractions while the animals were under general anesthesia. Axial eye dimensions were measured with A-scan ultrasound with a 33 MHz transducer (Troilo et al., 2000a). Axial length is expressed as the sum of the anterior chamber depth, lens thickness and vitreous chamber depth; it does not include retinal or choroidal thickness.

3. Results

3.1. Refractions, biometry and age

Refractions obtained from the COAS 2nd order Zernike coefficients and a 3-mm diameter pupil are compared in Fig. 1 to mean refractions obtained on the same day by retinoscopy and the Hartinger refractometer. The COAS refractions were well correlated with the mean of the retinoscopy and Hartinger refractions ($y = 0.8525x - 0.363$; $R^2 = 0.812$; $p < 0.0001$). Thus the COAS refractions tended to be more myopic than the white-light refractions by about 0.36 D. This difference between methods may be related to pupil diameter since the dilated pupil of many animals was greater than 3 mm. The minimum pupil diameter in the selected COAS images increased with age, ranging from about 3 mm in the youngest animals to about 3.8 mm in the oldest animals. The variation in minimum pupil diameter in mm against age in days was fit with the logarithmic function $y = 0.331 * \ln(x) + 2.035$; $R^2 = 0.687$.

For those animals that had large enough pupils in the COAS measurements, 2nd order refractions were calculated for 3.5 mm pupils and plotted against those for 3.0 mm pupils. Out of the 96 measurement sessions, there were 72 sessions that had pupils large enough for this analysis. The resulting linear regression was $y = 1.0492x + 0.3151$; $R^2 = 0.9757$, where y is the COAS 3.5-mm pu-

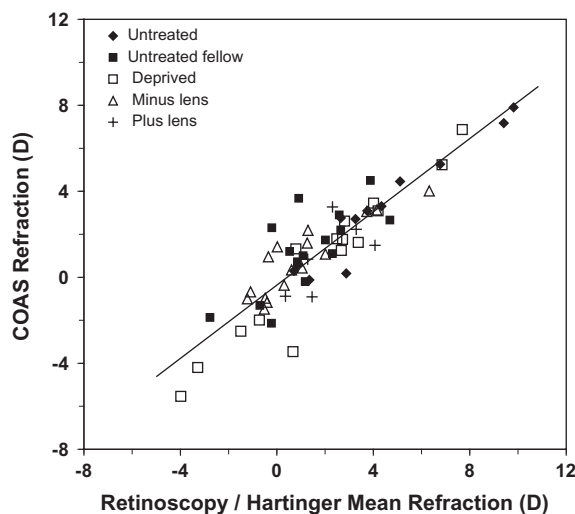


Fig. 1. Spherical equivalent refractions, in Diopters, obtained for 3-mm pupils from the COAS aberrometer, plotted against the mean of the spherical equivalent refractions obtained from retinoscopy and the Hartinger coincidence optometer. Measurements were performed on the same day on both eyes of 16 subjects; measurements from multiple sessions are included on six of the subjects, for a total of 64 measurements. Untreated eyes (filled diamonds) are data for four young subjects up to 51 days of age (two became monocular deprivation subjects). Data from untreated fellow eyes (filled squares) and form-deprived eyes (open squares) are shown for eight of the monocular deprivation subjects. Open triangles are data for five minus lens-treated subjects and plus signs are data for one positive lens-treated subject. Linear regression is fit to all data points: $y = 0.8525x - 0.363$; $R^2 = 0.812$; $p < 0.0001$.

pil refraction and x is the COAS 3-mm pupil refraction, both in Diopters. This indicates that an increase in pupil diameter of 0.5 mm results in a refraction shift toward hyperopia of about $+0.32$ D. When we plotted the COAS 3.5-mm pupil refractions (y) against 49 available same-session retinoscopy and Hartinger refractions (x), the resulting linear regression was $y = 0.8412x - 0.0751$; $R^2 = 0.6549$. This y -intercept indicates better agreement between methods for refractions. It is likely that the retinoscopy refractions were dependent upon the pupil diameter, since the Hartinger instrument has a fixed distance between the measurement beams in the pupil.

Marmosets generally were hyperopic at the youngest ages and became more myopic with age, consistent with previous studies of refraction development in marmosets (Graham & Judge, 1999; Troilo & Judge, 1993). Fig. 2 shows COAS refractions for untreated eyes as a function of age. The filled diamonds represent the refractions from both eyes of six experimental animals before they began the treatment phase, and the open diamonds represent data for the fellow untreated eyes of the monocular deprivation animals during the treatment phase. The filled triangles represent data on the two binocularly untreated animals at the age of 18 days and again at age 51 days; data for the latter age are shown since they overlap slightly with the treatment phase. Refractions leveled off at about -2.00 D of myopia at just over 100 days of age and the data can be fit well with a logarithmic function, provided in the figure caption.

Axial length and vitreous chamber depth increased with age in untreated eyes. For the age range from 30 to 122 days, axial length, in mm, increased with age in days according to the following logarithmic function: $y = 1.0514 \ln(x) + 4.731$; $R^2 = 0.714$. Vitreous chamber depth, in mm, increased with age in days by: $y = 0.7915 \ln(x) + 2.319$; $R^2 = 0.738$. Corneal radius of curvature, in mm, also increased with age in days in the untreated eyes by: $y = 0.1319 \ln(x) + 2.807$; $R^2 = 0.450$.

Cross-sectional refraction data are compared to vitreous chamber depth (Fig. 3a) and corneal radius of curvature (Fig. 3b) for the treatment phase from 51 to 102 days of age. Data are shown for the two binocularly untreated animals (filled diamonds), six monocular deprivation subjects (open and filled squares), three negative lens-treated subjects (triangles) and one positive lens-treated sub-

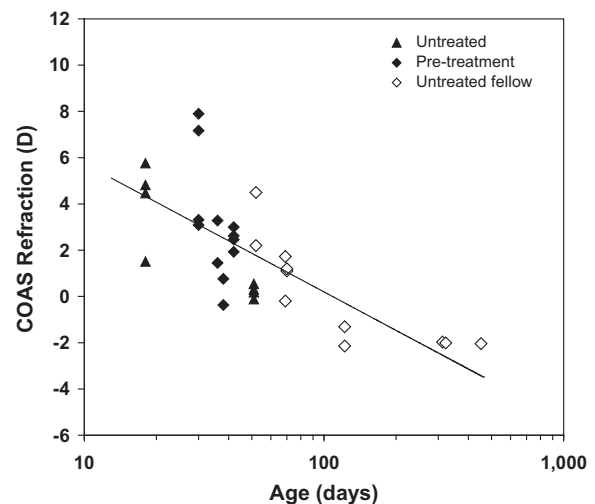


Fig. 2. Spherical equivalent refractions, in Diopters, obtained from the COAS aberrometer for 3-mm pupils, plotted against the subject age in days. Filled diamonds are data for untreated eyes of six experimental animals in the pre-treatment phase and open diamonds are data for untreated fellow eyes of the 11 monocularly untreated subjects. Filled triangles are longitudinal data from the two binocularly untreated animals. Logarithmic curve is fit to all data points: $y = -2.416 \ln(x) + 11.551$; $R^2 = 0.587$.

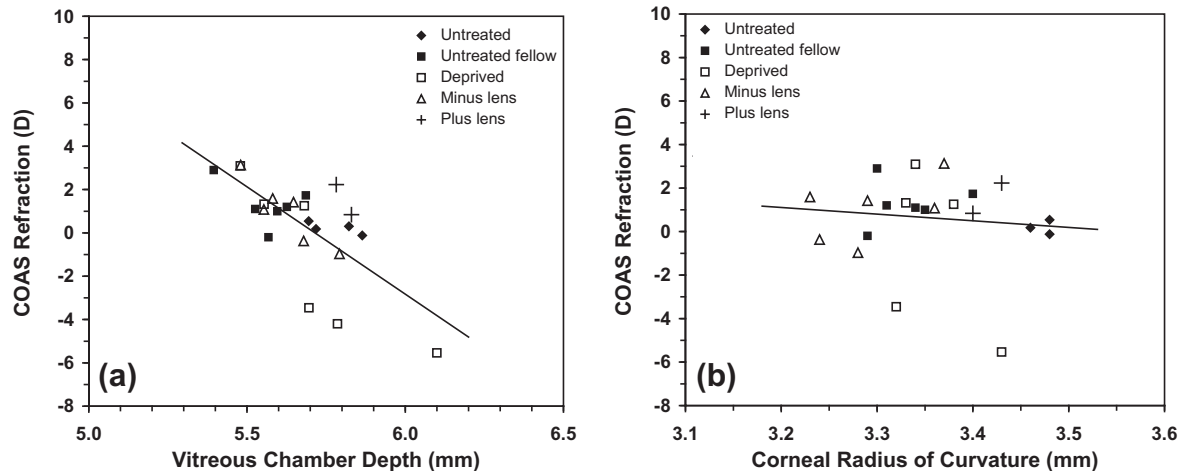


Fig. 3. Spherical equivalent refractions, in Diopters, obtained from the COAS aberrometer for 3-mm pupils, plotted against (a) vitreous chamber depth in mm or (b) corneal radius of curvature in mm, for various subjects during the treatment phase of study. Filled diamonds depict data from the two binocularly untreated animals at age 51 days; filled squares and open squares are data from the untreated fellow eyes and form-deprived eyes, respectively, of six monocular deprivation subjects at ages 66–70 days; open triangles depict data from both eyes of three negative-lens reared animals at ages 64–70 days; plus signs are data from both eyes of a positive lens-treated animal at age 102 days. One measurement is shown for each eye; corneal curvature data were not available from one eye of the untreated animals and one of the form-deprived eyes. Linear regression in each panel is fit to all data points. Regression in panel (a) is: $y = -9.909x + 56.627$; $R^2 = 0.4953$; $p = 0.00012$; regression in panel (b) is: $-3.3068x + 10.925$; $R^2 = 0.0121$; $p > 0.05$.

ject (plus symbols). The untreated animals were 51 days of age and tended to have longer vitreous chamber depths for their age, although their corneas were also flatter than those of the experimental animals; hence the untreated animals were nearly emmetropic. Our sample of treated eyes is small and the outcomes variable, but the highest amount of myopia was induced by monocular deprivation (open squares) and this was associated with increased vitreous chamber depth. A linear regression is fit through all of the data, and indicates a significant relationship of refraction to vitreous chamber depth in this age range ($p = 0.00012$). However, refraction showed no relationship to corneal curvature ($p > 0.05$). Vitreous chamber depths and refractions were similar in the lens-treated eyes and the untreated fellow eyes of the monocular deprivation subjects.

3.2. Higher-order wavefront aberrations in untreated eyes

Overall higher-order aberration (HOA) decreased with age in untreated eyes, as shown in Fig. 4. Fig. 4a shows the HOA wavefront error, in microns, combined from the 3rd through 7th Zernike orders, for eight individual subjects over ages from 18 to 51 days. Results for the experimental animals are shown during the period before treatment began. Subjects 1 and 2 are the binocularly untreated animals; subjects 3 through 6 became lens-treated animals, and subjects 7 and 8 became monocular deprivation animals. Longitudinal data are shown for subjects 1 and 2 at 18 and 51 days, and for subjects 7 and 8, at 30 and 38 days. The aberrations are shown for a 3-mm diameter pupil, with the exception of the larger gray symbols, in the upper right-hand area, that depict HOA aberration for a 3.5-mm diameter pupil in subjects 1 and 2. Data for the 3-mm pupil diameter were fit with a logarithmic function provided in the figure caption. There is a trend for aberration to decrease with age for a fixed pupil size. The data for subjects 1 and 2 suggest that the HOA aberration approximately scales with increasing eye size during this early growth period, since aberration for the 3.5 mm pupil diameter at 51 days is similar to the 3 mm pupil diameter at the youngest age.

Fig. 4b shows the HOA in microns for the untreated fellow eyes of subjects 7 and 8 over the period from 30 to 108 days of age. Data are shown for both 3 mm pupils (filled symbols) and 3.5 mm pupils

(open symbols). In addition, post-treatment data are shown for the untreated fellow eyes of two other monocular deprivation subjects (9 and 10, shown as squares and triangles). HOA decreases markedly over this period for fixed pupil diameters, such that aberrations for a 3.5-mm diameter pupil eventually match those of the 3-mm pupil at the younger ages. This is further evidence that aberrations may approximately scale with eye growth during this phase of development. Cross-sectional HOA data on untreated eyes for three pupil diameters are shown in Fig. 4c, using a 3-mm diameter pupil for ages up to 42 days, a 3.5-mm diameter pupil during the range from 69 to 122 days, and a 4-mm diameter pupil at ages near 320 days. These pupil diameters represent the approximate dilated pupil diameter for those age ranges. The higher-order aberration remains fairly constant over the growth period during the first year, when the aberration is scaled to the approximate dilated pupil diameter. The average for the 3-mm pupil was $0.253 \mu\text{m} \pm 0.062$ s.d., the average for the 3.5-mm pupil was $0.266 \mu\text{m} \pm 0.087$ s.d., and the average for the two eyes with a 4-mm pupil was $0.313 \mu\text{m} \pm 0.029$ s.d. The overall average HOA for the data in Fig. 4c was $0.265 \mu\text{m} \pm 0.065$ s.d.

3.3. Higher-order wavefront aberrations - age effect in treated and untreated eyes

The HOA wavefront error, combined from the 3rd through 7th Zernike orders for a 3-mm diameter pupil, is plotted as a function of age in days in Fig. 5a for both treated and untreated eyes. Cross-sectional results are shown for the treatment and post-treatment phases beyond 50 days of age. Data from the 11 monocular deprivation animals are shown for both the untreated fellow eye (filled diamonds) and the form-deprived eye (open squares). Results from both eyes of the lens-treated animals are shown; nine had worn negative lenses (open triangles) and one had worn positive lenses (plus symbols). Logarithmic functions were fit to the results during the treatment and post-treatment phases for the untreated fellow eyes (solid line), deprived eyes (dashed line) and minus lens-treated eyes (dotted line); parameters of these regressions are listed in Table 1. For comparison, cross-sectional aberration data from both eyes of eight young marmosets are shown before the treatment phase began (open

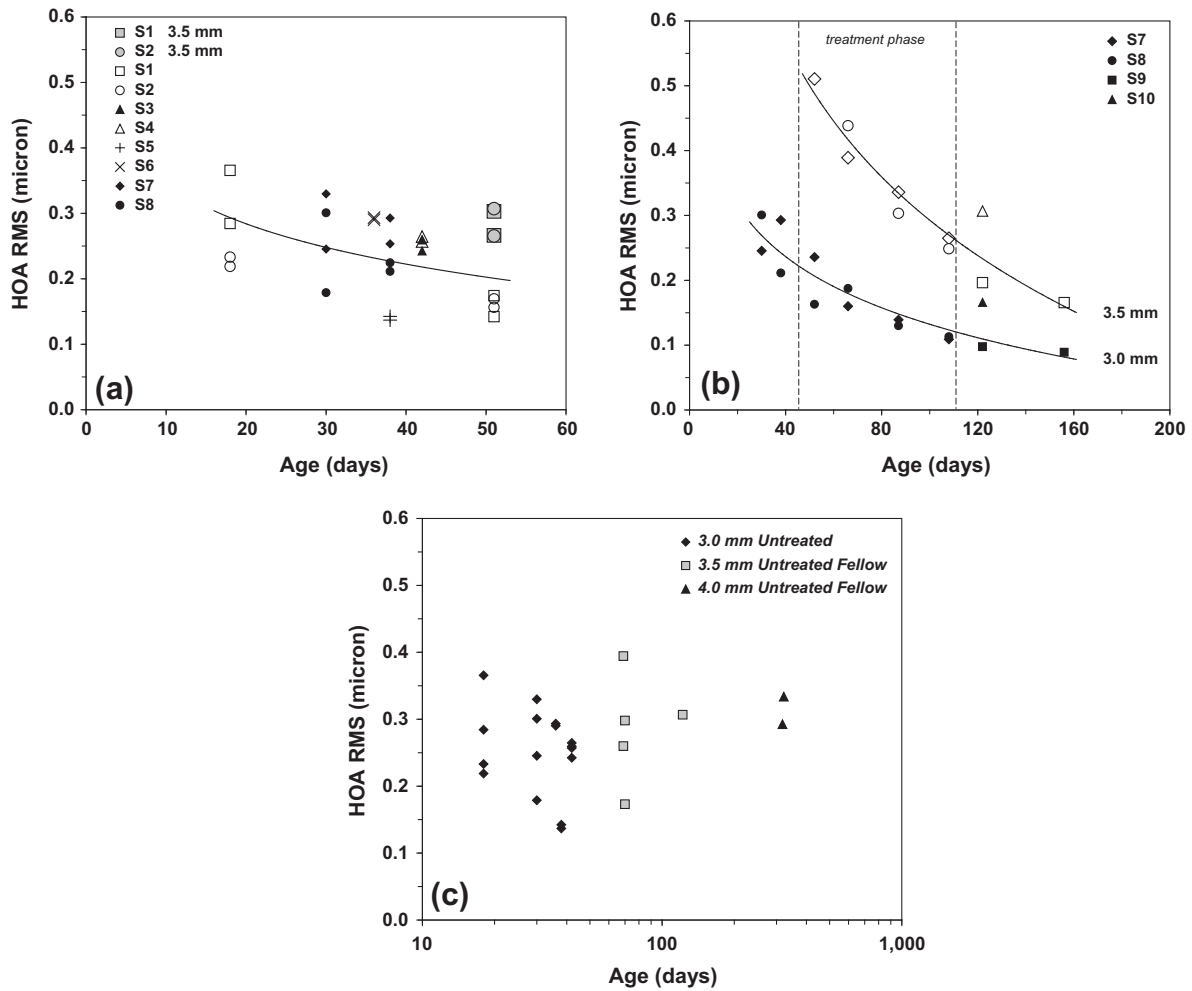


Fig. 4. Higher-order wavefront error in the third through seventh Zernike orders, in microns, plotted as a function of age in days on untreated eyes. (a) Results for eight individual subjects are shown for the period up to 51 days of age, before treatment began on the experimental animals. Subjects 1 and 2 were non-experimental animals, subjects 3–6 became lens-treated animals (subject 5 would become positive lens-treated while subjects 3, 4 and 6 became negative lens-treated) and subjects 7 and 8 became monocular deprivation animals. Wavefront error is shown for a 3-mm pupil diameter, with the exception of the larger symbols in gray for subjects 1 and 2, which are for a 3.5 mm pupil diameter. Logarithmic function is fit to only the 3-mm pupil data: $y = -0.089 \ln(x) + 0.551$; $R^2 = 0.228$. (b) Higher-order wavefront error, in microns, plotted as a function of age in days for the untreated fellow eyes of monocular deprivation animals. Results for subjects 7 and 8 are shown as filled diamonds and circles, respectively, for a 3-mm pupil diameter and open diamonds and circles for a 3.5 mm pupil diameter. Data for the 3.5 mm pupil are not shown for subject 8 at 52 days of age, since its pupil diameter was less than 3.5 mm. The treatment phase is marked by the vertical dashed lines. Data for the untreated fellow eyes of two other monocular deprivation animals (subjects 9 and 10) are also shown during the post-treatment phase, filled squares and triangle for a 3 mm pupil diameter, and open squares and triangle for a 3.5-mm pupil diameter. Logarithmic functions are fit to all of the subject data for each pupil diameter. The function for the 3-mm pupil is: $y = -0.114 \ln(x) + 0.656$; $R^2 = 0.811$, and the function for the 3.5 mm pupil is: $y = -0.299 \ln(x) + 1.669$; $R^2 = 0.903$. (c) Higher-order wavefront error, in microns, plotted as a function of age in days for untreated eyes; each data point represents a different eye. Filled diamonds represent the results on both eyes of the same 8 young marmosets shown in panel (a) for a 3-mm diameter pupil; gray squares represent data with a 3.5-mm diameter pupil from the untreated fellow eyes of five different monocular deprivation subjects; filled triangles represent data with a 4-mm diameter pupil from the untreated fellow eyes of two other monocular deprivation subjects in the post-treatment phase.

diamonds). These are the same subjects whose data were shown in Fig. 4a. The results indicate that aberrations continue to decrease with age at a fixed pupil size, even during the treatment phase. However the form-deprived eyes of the monocular deprivation subjects tend to have higher HOA than other eyes during the treatment and post-treatment phases.

Aberrations for a 3-mm diameter pupil in the individual 3rd through 6th Zernike orders are shown as a function of age in Figs. 5b–e. Eyes are the same in these panels as in Fig. 5a, and all panels use the same legend. Aberrations in the individual Zernike orders decreased with age through the treatment and post-treatment phases. Form-deprived eyes showed relatively more aberrations in the 3rd and 5th orders than eyes in other groups, while their 4th and 6th order aberrations were similar to those of their fellow untreated eyes. Young eyes in the pre-treatment phase showed relatively more aberrations in the 4th order than animals in the treatment phase.

Results for Zernike coefficient Z_4^0 (spherical aberration) are shown in Fig. 5f. Spherical aberration tended to be negative in young marmoset eyes before the treatment phase and this aberration trended toward zero with increasing age. The minus lens-treated eyes showed negative spherical aberration during the early phase of treatment that became less negative with increasing age, while the two positive lens-treated eyes had positive spherical aberration during the treatment phase (shown here at age 66 days; the two data points were nearly identical). However the positive lens-treated animal had a 4,0 coefficient near zero at age 38 days in the pre-treatment phase, while the negative-lens reared animals available during the pre-treatment phase had 4,0 coefficients near $-0.2 \mu\text{m}$. Thus there is a pattern during the initial lens rearing period of the 4,0 coefficient shifting in the less negative or positive direction relative to the pre-treatment values. Spherical aberration in both eyes of the monocular deprivation animals tended to be variable in the early treatment phase but trended toward zero with increasing age.

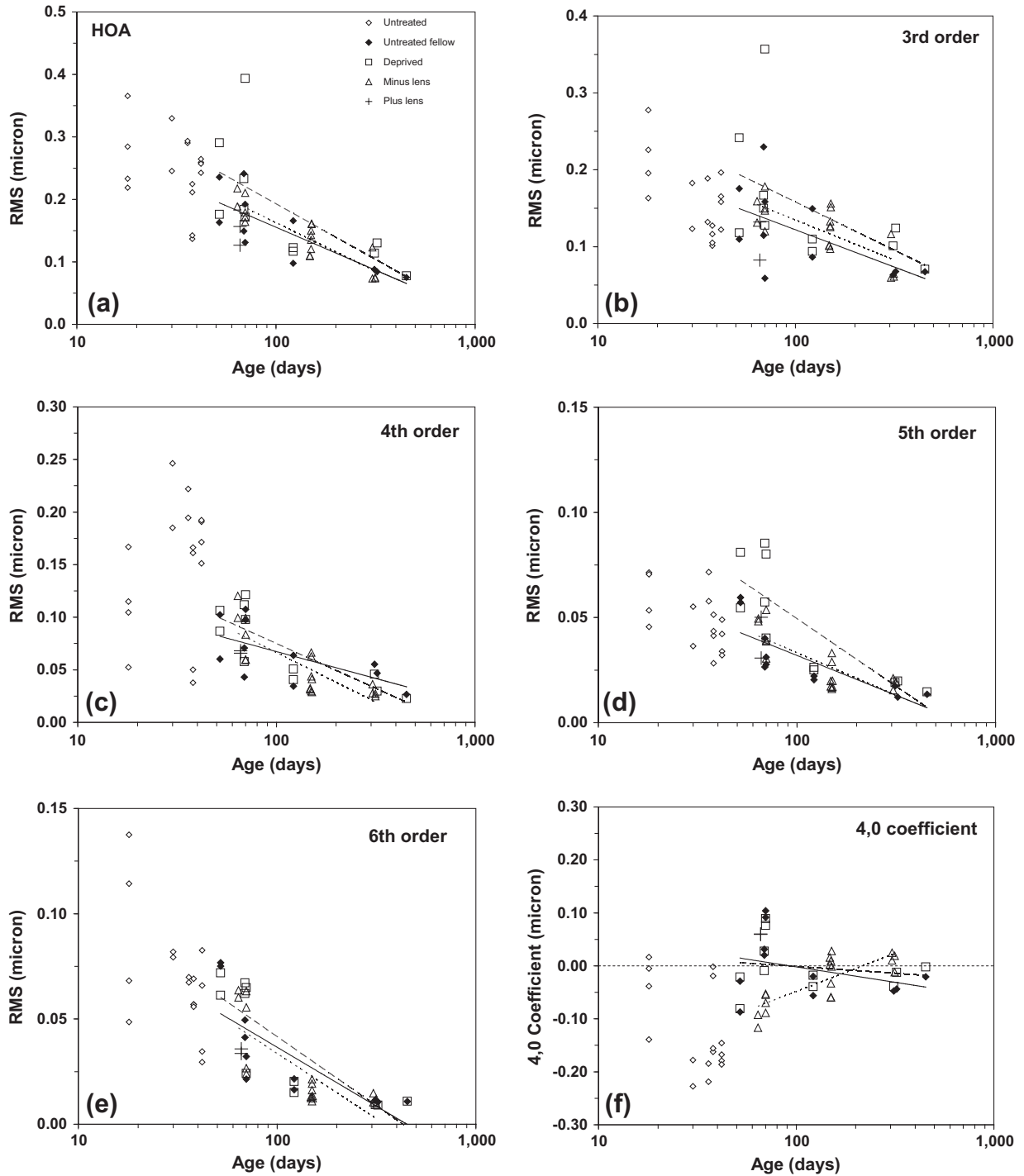


Fig. 5. Wavefront aberration error for a 3-mm diameter pupil, in microns, plotted against subject age in days on a logarithmic scale. The same legend is used for each panel. Results are shown for (a) RMS higher-order aberrations (HOA) in the third through seventh Zernike orders; (b) third order RMS; (c) fourth order RMS; (d) fifth order RMS; (e) sixth order RMS; and (f) the spherical aberration Z_4^0 coefficient. Open diamonds are cross-sectional data on both eyes of the eight young marmosets whose HOA data were shown in Fig. 4a. Results on the experimental animals in the treatment and post-treatment phases are cross-sectional. Data for both eyes of the 11 monocular deprivation animals are shown as filled diamonds for the untreated fellow eyes and open squares for the form-deprived eyes. Data for subjects 7 and 8 in Fig. 4b are shown here during the treatment phase at age 52 days. Results from both eyes of nine minus lens-treated animals are shown as open triangles, while the eyes of a single positive lens-treated animal are shown as plus signs. A logarithmic function of the form, $y = \text{slope} + \text{Ln}(x) + \text{intercept}$, is fit to the untreated fellow eyes (solid line), the form-deprived eyes (dashed line) and the minus lens-treated eyes (dotted line) during the treatment and post-treatment phases; parameters of the curve fit equations and correlation r values are given in Table 1.

3.4. Higher-order wavefront aberrations – treatment effect

Fig. 6 shows an example of the longitudinal study of wavefront aberrations in both eyes of one monocularly deprived animal (subject 8). The right eye wore an occluder starting at age 41 days and

the contralateral eye was left untreated. Data are shown for the pre-treatment session at age 38 days (top row), and for three sessions during treatment at ages 66, 87 and 106 days. Maps and data for the pre-treatment session are shown for a 3-mm diameter pupil; this is the largest pupil diameter for which aberrations could

Table 1

Logarithmic curve fit parameters, for equations of the form: $y = \text{slope} * \ln(x) + \text{intercept}$, where y is the RMS or coefficient value in microns and x is the age in days, for the data in Fig. 5a–f. Slopes and intercepts are given in the second and third columns, respectively, while correlation r values are given in the fourth column. Values for the untreated fellow eyes and the form-deprived eyes of the monocular deprivation animals correspond to the solid lines and dashed lines, respectively, in Fig. 5; values for the minus lens-treated eyes correspond to the dotted lines in Fig. 5.

Aberration order or coefficient	Slope	Intercept	r
Higher-order aberration (Fig. 5a)			
Untreated fellow	−0.0597	0.4302	0.7986
Deprived	−0.0773	0.5489	0.6592
Minus lens	−0.0676	0.4741	0.8882
3rd order (Fig. 5b)			
Untreated fellow	−0.0421	0.3157	0.5947
Deprived	−0.0543	0.4082	0.5225
Minus lens	−0.0452	0.3430	0.7526
4th order (Fig. 5c)			
Untreated fellow	−0.2220	0.1696	0.6336
Deprived	−0.0370	0.2454	0.8219
Minus lens	−0.0409	0.2546	0.8039
5th order (Fig. 5d)			
Untreated fellow	−0.0165	0.1079	0.8006
Deprived	−0.0280	0.1782	0.8107
Minus lens	−0.0176	0.1145	0.7954
6th order (Fig. 5e)			
Untreated fellow	−0.0243	0.1487	0.7819
Deprived	−0.0285	0.1728	0.8329
Minus lens	−0.0269	0.1577	0.7812
4,0 coefficient (Fig. 5f)			
Untreated fellow	−0.0253	0.1146	0.3282
Deprived	−0.0112	0.0503	0.1755
Minus lens	0.0625	−0.3361	0.7913

be computed in this young eye. For the three measurements during treatment, maps and data are shown for 3.5-mm pupils. Higher-order wavefront error maps were reconstructed from the 3rd through 7th order Zernike coefficients, and maps are all shown on the same $\pm 1 \mu\text{m}$ scale. Wavefront maps in the left column are for the form-deprived right eye and maps in the middle column are for the untreated left eye. Bar graphs in the right column show the relative ratio (right eye/left eye) of aberrations for the Z_3^{-3} trefoil and Z_4^0 spherical aberration Zernike terms. Before treatment, both eyes exhibit the negative spherical aberration characteristic of young marmoset eyes. During treatment, the occluded eye developed relatively more trefoil but less spherical aberration than the fellow eye. Fig. 7 shows the change in trefoil and spherical aberration coefficients over age in the occluded (open symbols) and untreated (filled symbols) eyes of this animal for both 3 and 3.5-mm diameter pupils; the arrow indicates the beginning of the treatment phase. Before treatment, both eyes show similar amounts of trefoil and spherical aberration, but after treatment, the occluded eye shows consistently more trefoil even while the trefoil aberration decreases during the treatment phase with increasing age. Spherical aberration is negative and of similar magnitude in both eyes and decreases with age.

Fig. 8 shows the average RMS wavefront error for different Zernike orders, as well as Zernike coefficients Z_3^{-3} and Z_4^0 , for different treatment groups. Averages for each group are based on single measurements per eye. Results are shown for the untreated fellow eyes (black bars) and form-deprived eyes (striped bars) of the 11 monocular deprivation animals, and for both eyes of the 10 lens-treated animals (stippled bars). Data were restricted to ages greater than 60 days, during the treatment and post-treatment phases; the average ages of the monocular deprivation and lens-treated animals were similar (162 vs. 149 days, respectively) and not significantly different in a t -test. The form-deprived eyes of the monocular deprivation animals tended to have greater amounts of

aberrations than their untreated fellow eyes. Aberrations in form-deprived eyes showed the greatest relative increase in the 3rd, 5th and 7th Zernike orders, which contain the asymmetric aberrations. Aberrations in the 5th and 7th orders, as well as trefoil aberration (Z_3^{-3}), were significantly higher in form-deprived eyes than in their untreated fellow eyes ($p < 0.05$ in paired t -test). Lens-treated eyes did not show significantly elevated amounts of aberrations compared to untreated eyes, except in the Z_3^{-3} trefoil term ($p < 0.05$ in t -test). The Z_3^{-3} trefoil coefficient was increased by about the same amount in both the lens-treated and form-deprived eyes. The other trefoil coefficient, Z_3^3 , was not significantly different among the groups of eyes. Lens-treated eyes showed more negative spherical aberration (Z_4^0 coefficient) than untreated or form-deprived eyes, but this difference did not reach significance. Since the two positive lens-treated eyes showed positive spherical aberration (Fig. 5f), we also compared only the eyes reared with minus lenses to the untreated eyes. The average Z_4^0 coefficient was more negative in the minus lens-treated eyes ($-0.0294 \mu\text{m}$) compared to the value for all lens-treated eyes ($-0.0205 \mu\text{m}$), but it was still not significantly different from that in the untreated eyes.

Lens-treated eyes had significantly more Z_2^2 vertical/horizontal astigmatism than the untreated fellow eyes (not shown in Fig. 8 due to the difference in scale). Lens-treated eyes had a mean \pm s.e.m. Z_2^2 astigmatism coefficient of $-0.242 \mu\text{m} \pm 0.094$ while that for untreated eyes was $0.093 \mu\text{m} \pm 0.057$ ($p = 0.019$ in t -test). The negative sign of the astigmatism coefficient indicates that the lens-treated eyes had with-the-rule astigmatism, or minus cylinder axis 180° . The form-deprived eyes had a larger range of the Z_2^2 astigmatism coefficient than their fellow untreated eyes, although the means were not significantly different (mean \pm s.e.m. was $-0.051 \mu\text{m} \pm 0.203$ for deprived eyes). We explored the correlation between 2nd order astigmatism coefficients and individual 3rd order coefficients of coma and trefoil since these coefficients could be associated with increased astigmatism if optical surfaces in an eye are misaligned.

In keeping with the recommended ANSI Z80.28 standard for reporting wavefront aberrations (American National Standards Institute (ANSI), 2010), we reversed the signs of coefficients from left eyes for Zernike terms that are asymmetric about the vertical midline (Z_2^2 , Z_3^1 , and Z_3^3). We first compared 3rd order coefficients to the Z_2^2 vertical/horizontal astigmatism term in all 46 eyes, with single measures per eye, but there was no significant correlation of any of the 3rd order terms with Z_2^2 astigmatism. For the individual groups shown in Fig. 8, the Z_3^3 trefoil coefficient decreased significantly with increasing Z_2^2 astigmatism in the form-deprived eyes ($y = -0.101x - 0.0273$; $R^2 = 0.470$; $p = 0.02$), while it had the opposite slope in the lens-treated eyes ($y = 0.0412x - 0.0152$; $R^2 = 0.227$; $p = 0.03$). This trefoil term was not correlated with Z_2^2 astigmatism in the untreated fellow eyes. The lens-treated eyes, probably due to their larger astigmatism, were the only group that showed correlations of other 3rd order terms with Z_2^2 astigmatism: lateral coma Z_3^1 ($p = 0.0498$) and Z_3^{-3} trefoil ($p = 0.04$) showed positive correlations with Z_2^2 astigmatism in the lens-treated eyes.

There were no significant differences in the average Z_2^2 oblique astigmatism coefficients among the groups in Fig. 8. However, when we compared 3rd order coefficients to the Z_2^2 oblique astigmatism in all 46 eyes, both the Z_3^{-3} trefoil term ($p < 0.0001$) and the Z_3^3 term ($p = 0.049$) increased with oblique astigmatism. For the individual groups of eyes shown in Fig. 8, only the lens-treated eyes ($p = 0.006$) and the form-deprived eyes ($p = 0.002$) had significant correlations of Z_3^{-3} trefoil term with oblique astigmatism. Untreated fellow eyes of the monocular deprivation animals did not show these effects. Thus the increased Z_3^{-3} trefoil observed in the form-deprived and lens-treated eyes in Fig. 8 is correlated with oblique astigmatism in those eyes. There was no significant

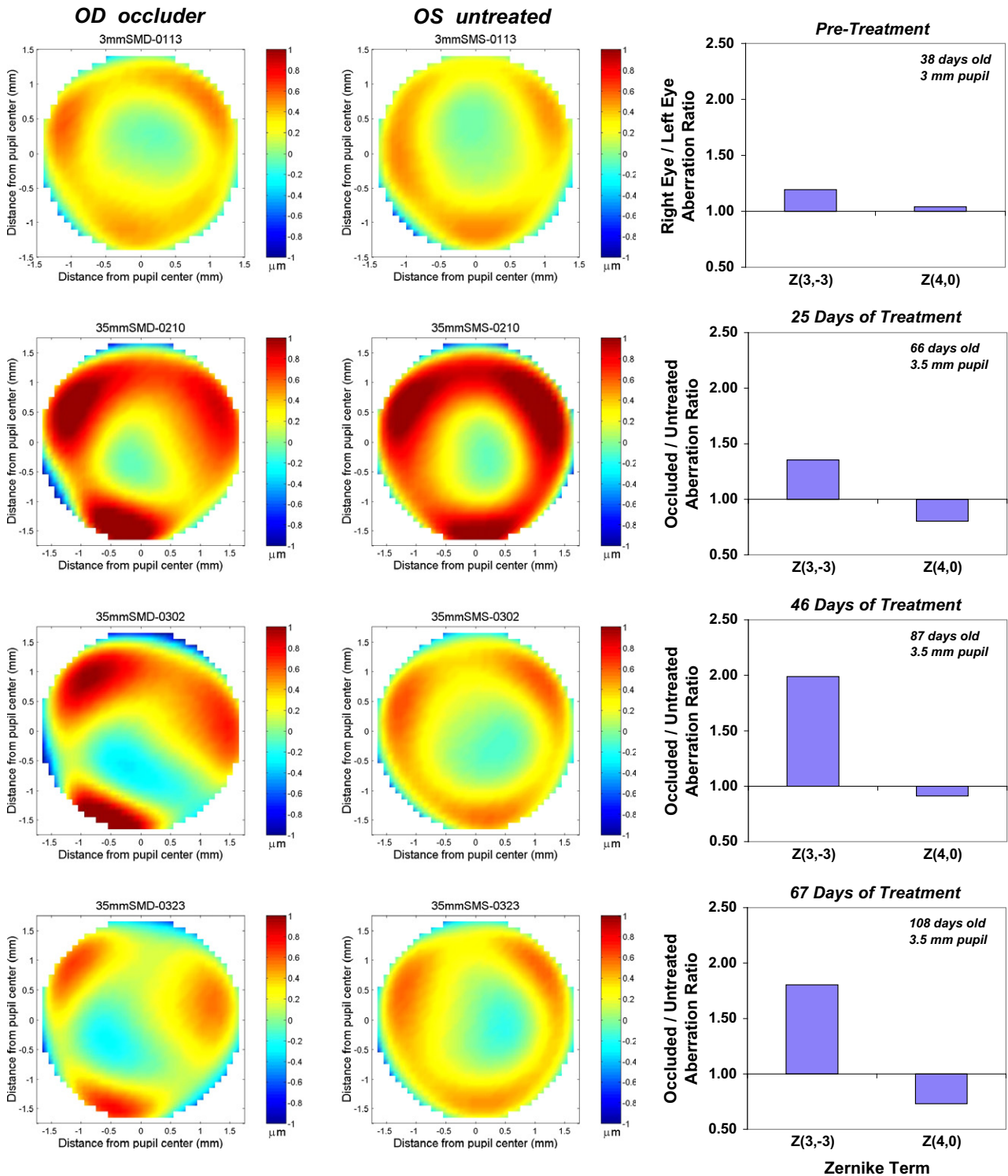


Fig. 6. Wavefront error maps for subject 8 who wore an occluder over the right eye during treatment that began at age 41 days. Wavefront maps in the left column are for the right eye and maps in the middle column are for the untreated left eye. Higher-order wavefront error maps were reconstructed from the 3rd through 7th order Zernike coefficients, and maps are all shown on the same $\pm 1 \mu\text{m}$ scale. Bar graphs in the right column show the relative ratio (right eye/left eye) of aberrations for the Z_3^3 trefoil and Z_4^4 spherical aberration Zernike terms. Data are shown for a 3-mm pupil diameter for the pre-treatment session at age 38 days (top row), and for a 3.5-mm diameter pupil for the three sessions during treatment at ages 66, 87 and 106 days.

correlation of the other trefoil term, Z_3^3 , with oblique astigmatism in the individual groups of treated or untreated eyes.

Comparing aberrations in the two eyes of the monocular deprivation animals, third-order aberrations were uncorrelated between eyes ($p = 0.70$), while aberrations in each of the 4th

through 7th orders were highly correlated ($p < 0.005$ for 4th, 5th and 6th orders; $p < 0.05$ for 7th order). The interocular correlation of 5th and 7th order aberrations persisted even though 5th and 7th order aberrations were significantly greater in the form-deprived eye (Fig. 8). This result implies that monocular

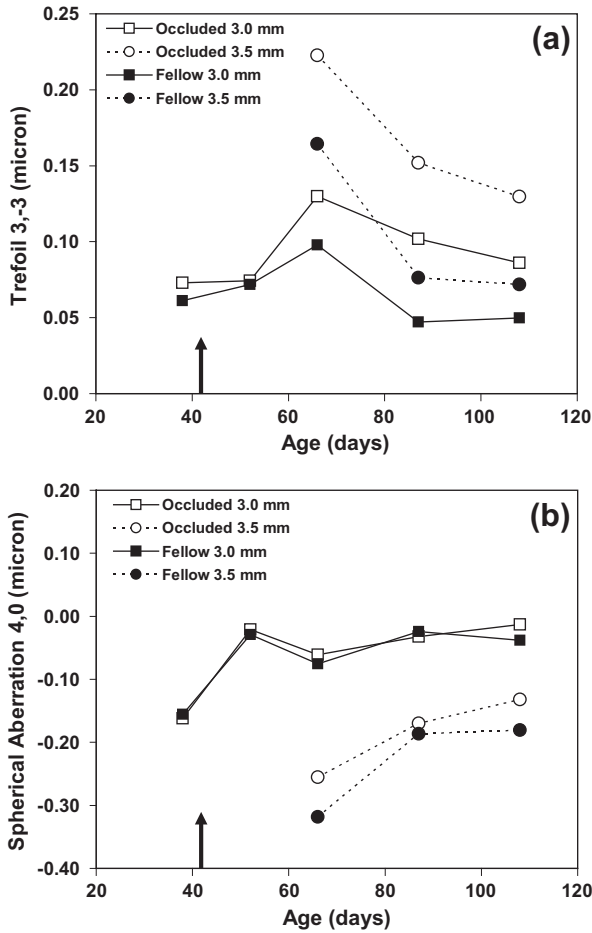


Fig. 7. Trefoil Z_3^{-3} coefficient (a) and spherical aberration Z_4^0 coefficient (b) plotted as a function of age in the occluded eye (open symbols) and the fellow untreated eye (filled symbols) of the subject in Fig. 6. Arrow indicates the start of occlusion of the right eye.

deprivation disrupts primarily the interocular correlation of the 3rd order aberrations.

3.5. Higher-order wavefront aberrations and relation to refraction and biometry

Younger untreated eyes were hyperopic (Fig. 2) and had higher RMS aberrations (Fig. 4), so it is not surprising that HOA in untreated eyes significantly increased with increasing hyperopia. When data from single measurements per untreated eye were combined, from all ages from 18 to 452 days, the linear regression of HOA in microns for a 3-mm pupil vs. COAS spherical equivalent refraction in Diopters was: $y = 0.0249x + 0.163$; $R^2 = 0.48$; $p < 0.001$. When ages were restricted to the range from 64 to 151 days, there was no significant relationship between HOA aberration magnitude and refraction in either the untreated or treated eyes (Fig. 9). This plot includes data from both eyes of eight of the monocular deprivation animals (filled diamonds and open squares), 14 eyes of seven of the minus lens-treated animals (triangles) and both eyes of the positive lens-treated animal (plus signs). The mean HOA in each of these groups was: $0.156 \mu\text{m} \pm 0.044$ s.d. for the untreated fellow eyes, $0.208 \mu\text{m} \pm 0.089$ s.d. for the form-deprived eyes, $0.159 \mu\text{m} \pm 0.034$ s.d. for the minus lens-treated eyes and $0.142 \mu\text{m} \pm 0.081$ s.d. for the plus lens-treated eyes.

Higher-order aberrations were related to eye size for ages greater than 50 days. Overall higher-order wavefront error for a 3-mm pupil decreased as the axial length increased

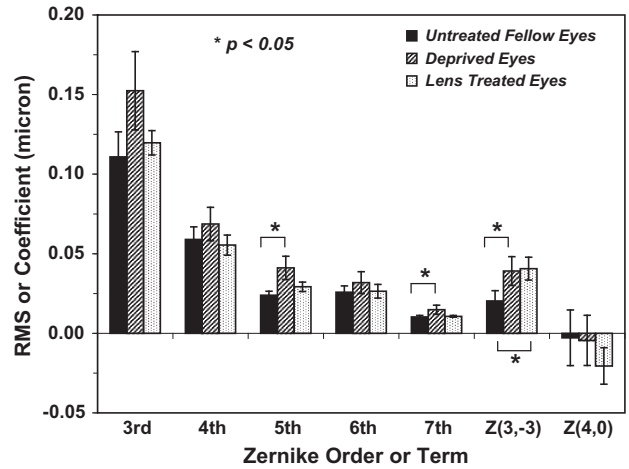


Fig. 8. Mean wavefront aberrations for a 3-mm diameter pupil, in micron, shown as RMS in each Zernike order and as the coefficient value for trefoil Z_3^{-3} and spherical aberration Z_4^0 . Eyes were in the treatment and post-treatment phases, and results are for a single measure per eye. Means are shown for the 11 untreated fellow eyes (solid bars) and the 11 form-deprived eyes (striped bars) of the monocular deprivation animals, and both eyes of the 10 lens-treated animals (stippled bars). Error bars are ± 1 s.e.m. Average ages of the monocular deprivation and lens-treated animals were similar (162 days vs. 149 days, respectively) and not significantly different. Deprived eyes had significantly greater aberrations in the 5th and 7th orders and significantly greater trefoil Z_3^{-3} than their untreated fellow eyes, based on paired *t*-tests. Lens-treated eyes also had significantly greater trefoil Z_3^{-3} aberration than the untreated eyes, based on a *t*-test.

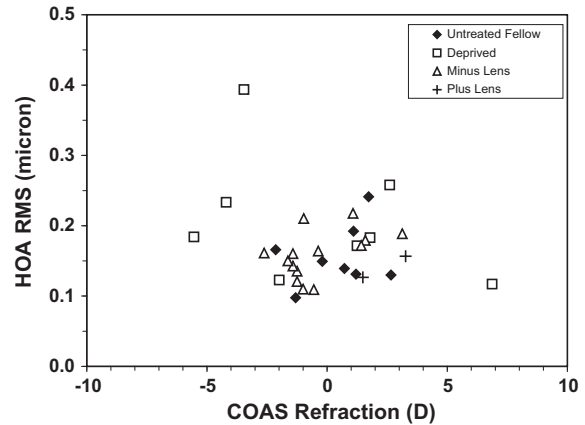


Fig. 9. Higher-order aberrations for a 3-mm diameter pupil, in microns, as a function of the COAS spherical equivalent refraction in Diopters during the age range from 64 to 151 days of age. Each data point is from single measurement on a given eye; results are shown from both eyes of eight of the monocular deprivation animals (filled diamonds and open squares), 14 eyes of seven of the minus lens-treated animals (triangles) and both eyes of the positive lens-treated animal (plus signs).

($y = -0.0615x + 0.7398$ where y is the HOA in micron and x is the axial length in mm; $R^2 = 0.34$; $p < 0.0001$) and as the cornea flattened ($y = -0.3133x + 1.2169$ where y is the HOA in micron and x is the corneal radius of curvature in mm; $R^2 = 0.15$; $p = 0.0043$). Similar effects were observed in the individual 3rd through 7th Zernike orders. These relationships are consistent with aging, however, because the aberrations decrease with age and both axial length and corneal radius of curvature increase with age. To avoid confounding effects of age, we compared interocular differences in aberrations and refractions in the monocular deprivation animals. Only 3 of the 11 animals in the monocular deprivation group had pronounced myopia in the occluded eye when they were examined in this study; of the remaining eight subjects, five were measured

after treatment had ceased, so their refractions may have recovered from the effects of deprivation. Form-deprived eyes that were relatively more myopic than their fellow eye showed significantly greater axial length ($y = -0.0559x - 0.0206$ where x is the interocular difference in refraction in Diopters and y is the interocular difference in axial length in mm; $R^2 = 0.74$; $p < 0.0001$). This regression is based on all 15 sessions in which biometric data were available for the monocular deprivation subjects. The more myopic eyes of the monocular deprivation subjects tended to exhibit greater aberrations than their fellow untreated eyes (Fig. 10). The interocular comparison is expressed as a difference in RMS aberration of the deprived eye minus that of the untreated eye, plotted against the interocular difference in refraction. One subject had developed almost 7 D of hyperopia in the form-deprived eye while its fellow eye was about 2 D myopic; hence this subject had an interocular difference in refraction of +9 D. Data for the 4th, 5th and 6th Zernike orders are shown in Fig. 10 for single sessions on each of the 11 monocular deprivation subjects. Linear regressions were significant in the 5th and 6th Zernike orders ($R^2 = 0.46$; $p = 0.022$ and $R^2 = 0.52$; $p = 0.012$, respectively). Fourth order aberrations were higher in the more myopic eyes but the regression was not significant ($R^2 = 0.21$). Higher-order and third-order aberrations also tended to increase in the more myopic eyes (not shown in Fig. 10 due to a relatively greater scale) but these trends were not significant. Form-deprived eyes that were relatively more myopic than their fellow untreated eye also tended to exhibit greater Z_3^{-3} trefoil aberration ($R^2 = 0.20$; $p > 0.05$).

3.6. Anesthesia effect

Fig. 11 illustrates the effect of anesthesia on wavefront aberrations for a 3-mm diameter pupil. Fourteen marmoset eyes were measured while the subjects were under general anesthesia. Aber-

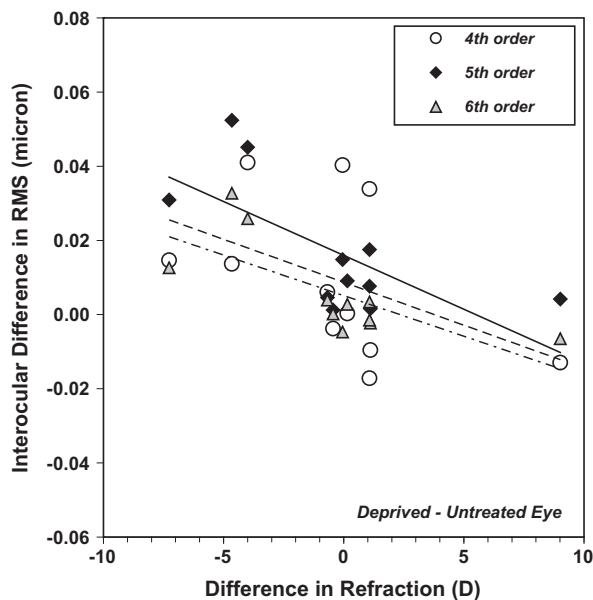


Fig. 10. Interocular difference in aberrations, in microns, as a function of the interocular difference in refraction, in Diopters, for the monocular deprivation subjects. The interocular comparison is expressed as the difference of the deprived eye value minus the untreated eye value. Data are shown for a single session for the 11 monocular deprivation animals. Interocular difference in RMS for the 4th Zernike order aberrations are shown as open circles, for the 5th order as filled diamonds and for the 6th order as gray triangles. Linear regression for the 4th order (dashed line): $y = -0.0023x + 0.009$; $R^2 = 0.21$, $p > 0.05$; 5th order (solid line): $y = -0.0029x + 0.0160$; $R^2 = 0.46$, $p = 0.022$; and 6th order (dash-dot line): $y = -0.0022x + 0.0051$; $R^2 = 0.52$, $p = 0.012$.

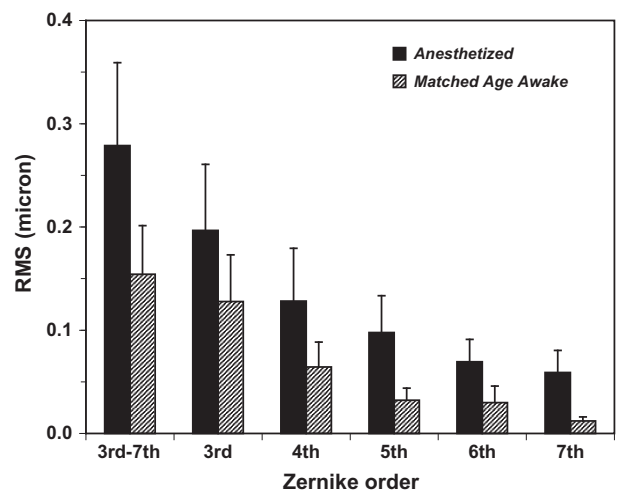


Fig. 11. Mean RMS wavefront aberration for a 3-mm diameter pupil, in micron, for the 3rd through 7th Zernike orders (left hand pair of bars) and for each Zernike order, for 14 eyes of seven experimental subjects (three monocular deprivation animals and four lens-treated animals). Solid bars depict data for subjects when anesthetized with Saffan, and striped bars depict data for the same number of age- and treatment-matched awake subjects. Error bars are 1 standard deviation.

rations in these eyes were measured again about 100 days later while the subjects were awake, but due to the dominance of age effects on aberrations, we compared the results with anesthesia to measurements on 14 eyes of seven other awake marmosets that were matched in age and treatment types to the group measured under anesthesia. Refractions of the anesthetized animals in the COAS were on average $+0.05 \text{ D} \pm 0.78 \text{ D s.e.m.}$ for a 3-mm pupil diameter, while the COAS refractions for the matched awake animals were on average $+1.19 \text{ D} \pm 0.47 \text{ D s.e.m.}$ The overall higher-order wavefront error is expressed as the RMS of the combined 3rd through 7th order terms; RMS wavefront error is also shown for each of the higher Zernike orders. Overall aberrations are significantly higher ($p < 0.01$) when the animals are anesthetized, for all Zernike orders. The HOA were increased by a factor of 1.8 under anesthesia relative to the awake condition, and there is a relatively larger effect of anesthesia on the higher Zernike orders, with the ratio of increased aberrations ranging from 1.5 in the 3rd order to 4.9 in the 7th order.

4. Discussion

4.1. Refractive error measurement

We found a good correspondence between the COAS measurement of spherical equivalent refractive error and the retinoscopy and Hartinger coincidence refractometer measurements. The COAS refractions in Fig. 1 are calculated using only the 2nd order Zernike terms and do not include the fourth order spherical aberration term, or Seidel sphere, often used to calculate refractions for human eyes (Salmon et al., 2003). We found that young marmoset eyes showed negative spherical aberration (Fig. 5f), so if we had included the spherical aberration term, that would have shifted the marmoset COAS refractions to even relatively higher amounts of myopia. We noted that the restriction of pupil size in the COAS refractions to 3 mm may have shifted those refractions to a relatively more myopic position, which is consistent with the negative spherical aberration observed in many marmoset eyes.

In the small eye, retinal reflection in white-light retinoscopy is thought to occur at the vitreous-retinal interface, which lies in front of the photoreceptor layer (Glickstein & Millodot, 1970). This effect creates a greater dioptric error relative to the photorecep-

tors, leading to a significantly more hyperopic refraction than that obtained using visual evoked potentials or other behavioral methods (Norton, Wu, & Siegwart, 2003). In this study, neither the retinoscopy and Hartinger refractions nor the COAS refractions were adjusted for the small eye artifact. The agreement between the white-light refractions and the COAS refractions for 3.5-mm pupils was somewhat surprising, because the small eye artifact is estimated to produce about 2.60 D of hyperopia in white-light retinoscopic measurements in the adult marmoset eye (Troilo, Howland, & Judge, 1993). The COAS instrument uses infrared (IR) light so the reflection should take place at a deeper retinal position compared to the white-light refraction, and this should have resulted in relatively more myopic refractions in the small eye. This is consistent with other observations in this laboratory, that white-light refractions in the marmoset are relatively hyperopic relative to refractions with an IR autorefractor (PowerRefractor, MultiChannel Systems, Germany). On the other hand, the COAS refraction in IR should also be affected by longitudinal chromatic aberration (LCA), which would shift the refraction toward more hyperopic values relative to white light. The COAS instrument uses a -0.71 D shift, which we retained in our measurements, to reference the IR refraction to a visible wavelength of 550 nm. This value is based on the LCA of the human eye (Howarth & Bradley, 1986; Llorente, Diaz-Santana, Lara-Saucedo, & Marcos, 2003). LCA is theoretically expected to be higher in the marmoset than in humans, due to their relatively steeper ocular surfaces, so the COAS LCA shift may be too low a correction for the marmoset eye. Uncompensated residual LCA, which would shift the refraction toward more hyperopic values, could have been compensated partially by the myopic shift due to the deeper retinal reflection in IR. This is consistent with a study in human infant eyes, about 2/3 the size of adult eyes, that reported that the chromatic difference of focus was not significantly higher in human infants with respect to that in adults (Wang, Candy, Teel, & Jacobs, 2008). The opposing relative contributions of these two factors, longitudinal chromatic aberration and the difference in reflection layer in visible vs. IR light, may have resulted in the good agreement between white-light and COAS refractions in the marmoset eye.

COAS measurements were typically performed under awake conditions while the retinoscopy and Hartinger measures were performed with the subjects under anesthesia. We found that the marmoset eye is more aberrated under anesthesia (Fig. 11); this agrees with results found in mice (Garcia de la Cera et al., 2006b). In the mouse, refractions were less hyperopic in the anesthetized state compared to the awake condition, consistent with the results of this study (Garcia de la Cera et al., 2006b). Our prior measurements of the effects of polymethyl methacrylate (PMMA) contact lenses on aberrations in marmosets indicate that disrupted tear film quality increases aberrations at the higher Zernike orders (Coletta et al., 2004). That implies that the increased aberrations in the anesthetized state are likely to be due to reduced tear film quality. Additional differences could potentially arise from changes in the crystalline lens (Garcia de la Cera et al., 2006b).

4.2. Refractive error response to treatment

Visually form-deprived eyes that were more myopic than their untreated fellow eyes also had relatively longer axial lengths, but not all form-deprived eyes became myopic. The magnitude of response to treatment and the interocular differences found across subjects varied among animals, as had been reported in earlier studies in marmosets (Troilo et al., 2000a). As all animals were treated at similar ages, the age-dependent susceptibility to myopia development cannot be invoked as a cause for the variation (Troilo & Nickla, 2005).

Refractive response to lens treatment was lower in magnitude than the average response to form deprivation. Since the animals were treated bilaterally with lenses, direct comparison with an untreated fellow eye is not possible, and therefore some effects could be masked by intersubject variability in biometry, keratometry, refraction and higher-order aberrations. Earlier studies on marmosets found that negative lenses tended to induce myopic error and positive lenses tended to induce hyperopic error, although the amount of induced refractive error does not appear well correlated with the treatment lens power (Troilo et al., 2007). In this study, 72% of the 18 eyes treated with negative lenses had a myopic COAS refractive error after the treatment period had ended. We speculate that the method of spectacle lens rearing, which involved fitting lenses in frames and mounting them over the marmoset eyes, may have imposed uncontrolled peripheral defocus or deprivation from the frames that may have affected the overall visual control of eye growth and produced different axial refractions. This possibility is supported by an earlier study using spectacle lenses, in which relative axial growth rates were modulated up by negative lenses and down by positive lenses, but the overall refractive states became more myopic compared to untreated eyes (Troilo & Nickla, 2000). More recently we have observed more consistent results using extended wear contact lenses to impose defocus (Troilo et al., 2009).

4.3. Decrease of aberrations during development

At a constant pupil size, we found a steady decrease of aberrations with development during infancy and adolescence in marmosets (Fig. 4a and b). The decrease in aberrations occurs for untreated eyes, as well as for both form-deprived and lens-treated eyes (Fig. 5). This decrease in aberrations parallels an increase in axial length, a decrease in corneal radius of curvature and a decrease of hyperopia during development. However, when the pupil diameter was increased with age to approximate the increase in eye size with development, aberrations remained fairly constant with age (Fig. 4c).

Other studies have reported a decrease in aberrations with age, for fixed pupil sizes, in several animal species and in humans. Garcia de la Cera et al. (2006a) and Kisilak et al. (2006) found an improvement in the optics during the first two weeks post-hatching in chickens, and Ramamirtham et al. (2007) also reported a decrease in higher-order aberrations in Rhesus monkeys during the first 200 days of age. The ocular aberrations in 5–7 week old human infants are only slightly worse than in adulthood, for different natural pupil diameters in each group (Wang & Candy, 2005). A cross-sectional study from 5.7 to 82.3 years of age reported a decrease in high order aberrations from childhood to adolescence and early adulthood in humans, for a constant pupil size of 5 mm (Brunette, Bueno, Parent, Hamam, & Simonet, 2003).

Interestingly, we found that treated eyes also demonstrate the decrease in aberrations with age and this agrees with studies on chickens (Garcia de la Cera et al., 2006a) and Rhesus monkeys (Ramamirtham et al., 2007). This finding supports a passive mechanism for the tuning of the optical components of the eye during development (Artal, Benito, & Taberner, 2006; Kelly, Mihashi, & Howland, 2004; Marcos, Rosales, Llorente, Barbero, & Jimenez-Alfaro, 2008). Unlike the tuning of axial length and optical power during emmetropization that requires proper retinal image quality, the improvement of optical quality with age is most likely not visually guided, as it also occurs in occluded eyes that have no visual feedback.

The decrease of aberrations with age, at a constant pupil size, may result from a passive geometrical mechanism. A very simple model of a growing eye supports a scaling of the wave aberrations with a factor inversely proportional to eye size (Howland, 2005).

More recently, eye growth models have been developed that predict age changes in retinal image blur, and these models could account for interspecies differences in the change of aberrations with age size (Hunter et al., 2009). A full understanding of the contributions of the different ocular components to optical quality of the eye and their change with aging can be achieved with more sophisticated computer eye models that include optical biometry, ocular misalignments and a full geometrical description of the ocular surfaces. Schematic models have been described for the marmoset eye (Troilo et al., 1993), mice (Schmucker & Schaeffel, 2004), guinea pigs (Howlett & McFadden, 2007), Rhesus monkeys (Lapuerta & Schein, 1995), and chickens (Irving, Sivak, Curry, & Callender, 1996). In most cases, these models describe only the paraxial properties of the eye. Predictions of higher-order aberrations have been achieved with very high accuracy in pseudophakic human eyes, using customized computer eye models that utilize fully known anatomical parameters (Rosales & Marcos, 2007; Tabernero, Piers, Benito, Redondo, & Artal, 2006). Lack of knowledge of surface asphericities, lens shapes and the gradient index of refraction has prevented the development of fully predictive schematic eyes for most experimental animal models, although plausible values of the unknown parameters may explain the change of aberrations with age and refractive error in chicks (Garcia de la Cera, 2008).

4.4. Relation of aberrations and refractive error

We found that form-deprived eyes showed greater amounts of higher-order aberrations than their untreated fellow eyes (Fig. 8). The differences were statistically significant, particularly in the asymmetric Zernike terms, while there were no differences in the spherical aberration term. In general, lens-treated eyes developed lower amounts of myopia compared to the form-deprived eyes and lens-treated eyes had higher-order aberrations that were similar in magnitude to the untreated eyes. Spherical aberration tended to be more negative in lens-treated eyes and only the Z_3^{-3} trefoil was significantly greater in lens-treated eyes than in untreated eyes.

Form deprived and lens-treated chicks and Rhesus monkeys in other studies (Garcia de la Cera et al., 2006a; Ksilak et al., 2006; Ramamirtham et al., 2007; Tian & Wildsoet, 2006) showed increased aberrations compared to untreated eyes (usually contralateral eyes in the chick studies and a control group in monkey studies). The fact that in our study the effects depend on the type of treatment may be due to the lower refractive response of the lens treatment or to intrinsic differences in the refractive error development between form deprivation and lens treatment. As in previous studies, our results suggest that the increase in aberrations is more likely to be a result of, rather than a cause for, myopia development. Ramamirtham et al. (2007) found that both myopia and hyperopia induction resulted in increased aberrations. In any case, the decreased optical quality produced by these increased aberrations is very minor, compared to the defocus blur introduced by the diffusers or the rearing lens blur. While the analysis of HOA vs. refraction may suggest lower amounts of aberrations in untreated eyes, and higher amounts in highly ametropic eyes, it is likely that age effects and/or overall eye size are confounding factors in this observation.

The Z_3^{-3} trefoil significantly increased in both form-deprived and lens-treated eyes (Fig. 8), and it tended to increase in proportion to the induced myopia in form-deprived eyes. The Z_3^{-3} trefoil term was correlated with oblique astigmatism in both the form-deprived and lens-treated eyes, and with vertical/horizontal astigmatism in the lens-treated eyes. These results suggest that treated eyes develop greater misalignment of optical surfaces than untreated eyes. The greater Z_3^{-3} trefoil aberration in treated eyes may involve a physical rather than a visually-guided process, since

it developed with both types of treatments in this study, form-deprivation and lens-induced defocus. Since the lens-treated eyes did not show increases in other 3rd, 5th and 7th order aberrations relative to untreated eyes, the increase in these other asymmetric aberrations in form-deprived eyes may be related to visual deprivation. Other studies also found that third-order aberrations changed very significantly with treatment (Garcia de la Cera et al., 2006a, 2007; Ramamirtham et al., 2007). It remains to be studied whether this change is a result of axial elongation, or rather a physical effect of the treatment with eye patches or goggles. For spherical aberration, we only found a non-significant tendency toward more negative values in lens-treated eyes (Fig. 8). In contrast with the consistent increase of third-order aberrations across studies, spherical aberration or 4th order RMS did not systematically change in all studies. Spherical aberration was about the same in lens-treated and untreated chick eyes and slightly more negative in form-deprived chick eyes (Garcia de la Cera et al., 2006a); however spherical aberration was significantly more positive in treated Rhesus monkey eyes (Ramamirtham et al., 2007).

4.5. Deprivation vs. lens-treatment

Visual form deprivation resulted in a different refractive error induction response and different higher-order aberrations (except for Z_3^{-3} trefoil) compared to lens rearing in marmosets. Previous literature showed less systematic refractive response in marmosets than in other species, such as Rhesus monkeys (Troilo & Nickla, 2005; Troilo et al., 2000b, 2007). Some differences may be related to the treatment protocols, which is monocular in the form-deprived animals and bilateral in the lens treatment. The lower amounts of aberrations found in the lens-treated eyes in comparison to form deprived eyes could be the result of the lower amounts of refractive error induced in that group.

4.6. Comparison to human eyes

The decrease of aberrations with age at a constant pupil size in the marmoset is qualitatively similar to previous findings in human eyes during childhood (Brunette et al., 2003). There also was a tendency for aberrations to be increased in marmoset eyes with induced myopia which is consistent with the general thought that ocular aberrations may increase in higher amounts of myopia in human eyes (Collins, Wildsoet, & Atchison, 1995; Marcos, Moreno-Barriuso, Llorente, Navarro, & Barbero, 2000; Paquin, Hammam, & Simonet, 2002). Some studies, however, have reported no increase in aberrations in lower amounts of myopia (Carkeet, Luo, Tong, Saw, & Tan, 2002; Cheng, Bradley, Hong, & Thibos, 2003). Other studies in humans have found differences in the optical aberrations of groups of myopes and hyperopes that are matched in age and refractive-error magnitude (Llorente, Barbero, Cano, Dorrnsoro, & Marcos, 2004). As the marmosets are used as an experimental model to better understand myopia in humans, it is interesting to relate their optical quality to that of humans. For approximately the same pupil size, the distribution and magnitude of the higher-order aberrations in marmosets are similar to that of humans infants (Wang & Candy, 2005). Marmosets had about 0.1 μm of higher-order aberration for a 3-mm pupil diameter, after nearly full development over the first year of life (Figs. 4b and 5). Human adult eyes with a 3-mm diameter pupil have lower higher-order aberrations, about 0.04 μm on average (Howland, 2002). However, the marmoset aberrations should be compared to human adult data for a 6-mm pupil diameter, which is closer to the scaled difference in axial length of the eyes; human eyes have about 0.3 μm HOA for a 6-mm diameter pupil (Howland, 2002). Another way to compare the marmoset eyes to adult human eyes is to estimate the effect of the higher-order wavefront aberration on retinal

image quality, using the equivalent defocus of the higher-order aberration (Thibos, Hong, Bradley, & Cheng, 2002). The equivalent defocus, M , is the amount of dioptric defocus that produces the same wavefront variance as the higher-order aberrations, and can be computed from the following formula:

$$M = 4\pi\sqrt{3} \left(\frac{\text{RMS error}}{\text{pupil area}} \right)$$

The equivalent defocus of 0.1 μm of higher-order aberration for a 3-mm pupil is 0.31 D. The equivalent defocus of the higher-order aberrations for a 6-mm pupil in an adult human eye is 0.21 D, measured for a large study population (Thibos et al., 2002). Thus, published values of higher-order aberration for adult human eyes suggest that the marmoset and human eyes may have similar optical quality, when taking into consideration the differences in eye size.

5. Conclusions

Higher-order aberrations in young marmosets decreased up to about 100 days of age for a fixed pupil diameter, but aberrations remained approximately constant with age if the pupil diameter was scaled to reflect the increasing pupil diameter during development. The magnitude of aberrations also varied with biometry in a manner consistent with age effects. Young marmoset eyes were characterized by negative spherical aberration which diminished after about 100 days of age. Asymmetric aberrations increased in marmoset eyes treated with monocular diffusers. Lens-treated and form-deprived eyes showed similar significant increases in Z_3^{-3} trefoil aberration, suggesting that the increase in this particular aberration may be related to factors that do not involve visual feedback, such as the physical presence of a goggle or lens. However, the increase in other odd-order (asymmetric) aberrations in form-deprived eyes may be due to lack of visual feedback because this effect was not evident in lens-treated eyes. Interocular comparisons of aberrations in monocularly deprived animals indicate that visual form-deprivation disrupts the interocular correlation of third-order aberrations. Overall higher-order RMS did not vary significantly with refractive error when ages were restricted to the treatment phase. However, form-deprived eyes that developed more myopia than their fellow untreated eyes also tended to show greater wavefront aberrations than their fellow untreated eyes.

Acknowledgments

The authors acknowledge technical assistance from Kristen Totonelly, Dr. Anne Moskowitz and Dr. Debora Nickla during various phases of this study. Supported by NIH Grants R01 EY011228 (DT), R01 EY012847 (NC) and R24 EY014817 (NC), Spanish MICINN FIS2008-02065 (SM), EURHORCS-ESF EURYI-05-102-ES (SM), and CSIC Programa de Movilidad (SM). The funding sources had no involvement in study design; in the collection, analysis and interpretation of data; in the writing of the report; and in the decision to submit the paper for publication.

References

American National Standards Institute (2010). ANSI Z80.28-2010. Ophthalmics – Methods of reporting optical aberrations of eyes. Washington, DC: American National Standards Institute.

Artal, P., Benito, A., & Taberner, J. (2006). The human eye is an example of robust optical design. *Journal of Vision*, 6(1), 1–7.

Atchison, D. A., Pritchard, N., & Schmid, K. L. (2006). Peripheral refraction along the horizontal and vertical visual fields in myopia. *Vision Research*, 46(8–9), 1450–1458.

Brunette, I., Bueno, J. M., Parent, M., Hamam, H., & Simonet, P. (2003). Monochromatic aberrations as a function of age, from childhood to advanced age. *Investigative Ophthalmology & Visual Science*, 44(12), 5438–5446.

Carkeet, A., Luo, H., Tong, L., Saw, S., & Tan, D. (2002). Refractive error and monochromatic aberrations in Singaporean children. *Vision Research*, 42, 1809–1824.

Charman, W. N., & Jennings, J. A. (1976). Objective measurements of the longitudinal chromatic aberration of the human eye. *Vision Research*, 16(9), 999–1005.

Cheng, X., Bradley, A., Hong, X., & Thibos, L. N. (2003). Relationship between refractive error and monochromatic aberrations of the eye. *Optometry and Vision Science*, 80(1), 43–49.

Coletta, N. J., Marcos, S., Wildsoet, C., & Troilo, D. (2003). Double-pass measurement of retinal image quality in the chicken eye. *Optometry and Vision Science*, 80(1), 50–57.

Coletta, N. J., Troilo, D., & Marcos, S. (2001). Optical quality of the marmoset eye. *Investigative Ophthalmology & Visual Science*, 42 [ARVO E-abstract, #S164].

Coletta, N. J., Troilo, D., Moskowitz, A., Nickla, D., & Marcos, S. (2003). Wavefront aberrations of the marmoset eye. *Investigative Ophthalmology & Visual Science*, 44 [ARVO E-abstract, #1987].

Coletta, N. J., Troilo, D., Moskowitz, A., Nickla, D., & Marcos, S. (2004). Ocular wavefront aberrations the awake marmoset. *Investigative Ophthalmology & Visual Science*, 45 [ARVO E-abstract, #4298].

Collins, M. J., Wildsoet, C. F., & Atchison, D. A. (1995). Monochromatic aberrations and myopia. *Vision Research*, 35(9), 1157–1163.

Diether, S., Gekeler, F., & Schaeffel, F. (2001). Changes in contrast sensitivity induced by defocus and their possible relations to emmetropization in the chicken. *Investigative Ophthalmology & Visual Science*, 42(12), 3072–3079.

García de la Cera, E. (2008). Optical quality and role of the ocular aberrations in animal models of myopia. Ph.D (p. 192). Valladolid: University of Valladolid.

García de la Cera, E. G., Rodríguez, G., de Castro, A., Merayo, J., & Marcos, S. (2007). Emmetropization and optical aberrations in a myopic corneal refractive surgery chick model. *Vision Research*, 47(18), 2465–2472.

García de la Cera, E. G., Rodríguez, G., Llorente, L., Schaeffel, F., & Marcos, S. (2006b). Optical aberrations in the mouse eye. *Vision Research*, 46(16), 2546–2553.

García de la Cera, E., Rodríguez, G., & Marcos, S. (2006a). Longitudinal changes of optical aberrations in normal and form-deprived myopic chick eyes. *Vision Research*, 46(4), 579–589.

Glickstein, M., & Millodot, M. (1970). Retinoscopy and eye size. *Science*, 168(931), 605–606.

Graham, B., & Judge, S. J. (1999). Normal development of refractive state and ocular component dimensions in the marmoset (*Callithrix jacchus*). *Vision Research*, 39(2), 177–187.

Howarth, P. A., & Bradley, A. (1986). The longitudinal chromatic aberration of the human eye, and its correction. *Vision Research*, 26(2), 361–366.

Howland, H. C. (2002). High order wave aberration of eyes. *Ophthalmic & Physiological Optics*, 22(5), 434–439.

Howland, H. C. (2005). Allometry and scaling of wave aberration of eyes. *Vision Research*, 45(9), 1091–1093.

Howland, H. C., Merola, S., & Basarab, J. R. (2004). The allometry and scaling of the size of vertebrate eyes. *Vision Research*, 44(17), 2043–2065.

Howlett, M. H., & McFadden, S. A. (2006). Form-deprivation myopia in the guinea pig (*Cavia porcellus*). *Vision Research*, 46(1–2), 267–283.

Howlett, M. H., & McFadden, S. A. (2007). Emmetropization and schematic eye models in developing pigmented guinea pigs. *Vision Research*, 47(9), 1178–1190.

Hung, L. F., Crawford, M. L., & Smith, E. L. (1995). Spectacle lenses alter eye growth and the refractive status of young monkeys[see comment]. *Nature Medicine*, 1(8), 761–765.

Hunter, J. J., Campbell, M. C. W., Ksilak, M. L., & Irving, E. L. (2009). Blur on the retina due to higher-order aberrations: Comparison of eye growth models to experimental data. *Journal of Vision*, 9(6:12), 1–20.

Irving, E. L., Sivak, J. G., Curry, T. A., & Callender, M. G. (1996). Chick eye optics: zero to fourteen days. *Journal of Comparative Physiology A – Sensory Neural & Behavioral Physiology*, 179(2), 185–194.

Kelly, J. E., Mihashi, T., & Howland, H. C. (2004). Compensation of corneal horizontal/vertical astigmatism, lateral coma, and spherical aberration by internal optics of the eye. *Journal of Vision*, 4(4), 262–271.

Ksilak, M. L., Campbell, M. C., Hunter, J. J., Irving, E. L., & Huang, L. (2006). Aberrations of chick eyes during normal growth and lens induction of myopia. *Journal of Comparative Physiology A – Sensory Neural & Behavioral Physiology*, 192(8), 845–855.

Lapuerta, P., & Schein, S. J. (1995). A four-surface schematic eye of macaque monkey obtained by an optical method. *Vision Research*, 35(16), 2245–2254.

Llorente, L., Barbero, S., Cano, D., Dorronsoro, C., & Marcos, S. (2004). Myopic versus hyperopic eyes: axial length, corneal shape and optical aberrations. *Journal of Vision*, 4(4), 288–298.

Llorente, L., Diaz-Santana, L., Lara-Saucedo, D., & Marcos, S. (2003). Aberrations of the human eye in visible and near infrared illumination. *Optometry and Vision Science*, 80(1), 26–35.

Lu, F., Zhou, X., Zhao, H., Wang, R., Jia, D., Jiang, L., et al. (2006). Axial myopia induced by a monocularly-deprived facemask in guinea pigs: A non-invasive and effective model. *Experimental Eye Research*, 82(4), 628–636.

Marcos, S., Moreno-Barruoso, E., Llorente, L., Navarro, R., & Barbero, S. (2000). Do myopic eyes suffer from larger amounts of aberrations? *Proceedings of the VIII International Conference in Myopia* (pp. 118–121). Boston.

Marcos, S., Rosales, P., Llorente, L., Barbero, S., & Jimenez-Alfaro, I. (2008). Balance of corneal horizontal coma by internal optics in eyes with intraocular artificial lenses: Evidence of a passive mechanism. *Vision Research*, 48(1), 70–79.

- Norton, T. T. (1990). Experimental myopia in tree shrews. *Ciba Foundation Symposium*, 155, 178–194 [discussion 194–179].
- Norton, T. T., & McBrien, N. A. (1992). Normal development of refractive state and ocular component dimensions in the tree shrew (*Tupaia belangeri*). *Vision Research*, 32(5), 833–842.
- Norton, T. T., Wu, W. W., & Siegwart, J. T. Jr., (2003). Refractive state of tree shrew eyes measured with cortical visual evoked potentials. *Optometry and Vision Science*, 80(9), 623–631.
- Paquin, M. P., Hamam, H., & Simonet, P. (2002). Objective measurement of optical aberrations in myopic eyes. *Optometry and Vision Science*, 79(5), 285–291.
- Ramamirtham, R., Kee, C. S., Hung, L. F., Qiao-Crider, Y., Huang, J., Roorda, A., et al. (2007). Wave aberrations in rhesus monkeys with vision-induced ametropias. *Vision Research*, 47(21), 2751–2766.
- Ramamirtham, R., Norton, T. T., Siegwart, J. T., & Roorda, A. (2003). Wave aberrations of tree shrew eyes. *Investigative Ophthalmology & Visual Science*, 44 [ARVO E-abstract, #1986].
- Rosales, P., & Marcos, S. (2007). Customized computer models of eyes with intraocular lenses. *Optics Express*, 15(5), 2204–2218.
- Salmon, T. O., West, R. W., Gasser, W., & Kenmore, T. (2003). Measurement of refractive errors in young myopes using the COAS Shack-Hartmann aberrometer. *Optometry and Vision Science*, 80(1), 6–14.
- Schaeffel, F., Burkhardt, E., Howland, H. C., & Williams, R. W. (2004). Measurement of refractive state and deprivation myopia in two strains of mice. *Optometry and Vision Science*, 81(2), 99–110.
- Schaeffel, F., & Howland, H. C. (1987). Corneal accommodation in chick and pigeon. *Journal of Comparative Physiology A*(160), 375–384.
- Schmucker, C., & Schaeffel, F. (2004). A paraxial schematic eye model for the growing C57BL/6 mouse. *Vision Research*, 44(16), 1857–1867.
- Smith, E. L., 3rd, Bradley, D. V., Fernandes, A., & Boothe, R. G. (1999). Form deprivation myopia in adolescent monkeys. *Optometry and Vision Science*, 76(6), 428–432.
- Smith, E. L., 3rd, Hung, L. F., & Harwerth, R. S. (1994). Effects of optically induced blur on the refractive status of young monkeys. *Vision Research*, 34(3), 293–301.
- Taberner, J., Piers, P., Benito, A., Redondo, M., & Artal, P. (2006). Predicting the optical performance of eyes implanted with IOLs to correct spherical aberration. *Investigative Ophthalmology & Visual Science*, 47(10), 4651–4658.
- Tejedor, J., & de la Villa, P. (2003). Refractive changes induced by form deprivation in the mouse eye. *Investigative Ophthalmology & Visual Science*, 44(1), 32–36.
- Thibos, L. N., Applegate, R. A., Schwiegerling, J. T. & Webb, R. (2000). Standards for reporting the optical aberrations of eyes. In V. Lakshminarayanan (Ed.), *Vision Science and Its Applications* (Vol. 35, pp. 232–244). *Trends in Optics and Photonics Series*. Washington, DC: Optical Society of America.
- Thibos, L. N., Hong, X., Bradley, A., & Cheng, X. (2002). Statistical variation of aberration structure and image quality in a normal population of healthy eyes. *Journal of the Optical Society of America*, 19(12), 2329–2348.
- Tian, Y., & Wildsoet, C. F. (2006). Diurnal fluctuations and developmental changes in ocular dimensions and optical aberrations in young chicks. *Investigative Ophthalmology & Visual Science*, 47(9), 4168–4178.
- Troilo, D., & Nickla, D. L. (2000). Visual regulation of eye growth and refractive state in a new world primate. In F. Thorn, D. Troilo, & J. Gwiazda (Eds.), *Myopia 2000: Proceedings of the VIII International Conference on Myopia* (pp. 170–174). Boston, MA: Myopia 2000, Inc.
- Troilo, D., Howland, H. C., & Judge, S. J. (1993). Visual optics and retinal cone topography in the common marmoset (*Callithrix jacchus*). *Vision Research*, 33(10), 1301–1310.
- Troilo, D., & Judge, S. J. (1993). Ocular development and visual deprivation myopia in the common marmoset (*Callithrix jacchus*). *Vision Research*, 33(10), 1311–1324.
- Troilo, D., Li, T., Glasser, A., & Howland, H. C. (1995). Differences in eye growth and the response to visual deprivation in different strains of chicken. *Vision Research*, 35(9), 1211–1216.
- Troilo, D., & Nickla, D. L. (2005). The response to visual form deprivation differs with age in marmosets. *Investigative Ophthalmology & Visual Science*, 46(6), 1873–1881.
- Troilo, D., Nickla, D. L., & Wildsoet, C. F. (2000a). Choroidal thickness changes during altered eye growth and refractive state in a primate. *Investigative Ophthalmology & Visual Science*, 41(6), 1249–1258.
- Troilo, D., Nickla, D. L., & Wildsoet, C. F. (2000b). Form deprivation myopia in mature common marmosets (*Callithrix jacchus*). *Investigative Ophthalmology & Visual Science*, 41(8), 2043–2049.
- Troilo, D., Quinn, N., & Baker, K. (2007). Accommodation and induced myopia in marmosets. *Vision Research*, 47(9), 1228–1244.
- Troilo, D., Totonelly, K., & Harb, E. (2009). Imposed anisometropia, accommodation, and regulation of refractive state. *Optometry and Vision Science*, 86(1), 31–39.
- Troilo, D., & Wallman, J. (1991). The regulation of eye growth and refractive state: An experimental study of emmetropization. *Vision Research*, 31(7–8), 1237–1250.
- Wallman, J., Wildsoet, C., Xu, A., Gottlieb, M. D., Nickla, D. L., Marran, L., et al. (1995). Moving the retina: Choroidal modulation of refractive state. *Vision Research*, 35(1), 37–50.
- Wallman, J., & Winawer, J. (2004). Homeostasis of eye growth and the question of myopia. *Neuron*, 43(4), 447–468.
- Wang, J., & Candy, T. R. (2005). Higher order monochromatic aberrations of the human infant eye. *Journal of Vision*, 5(6), 543–555.
- Wang, J., Candy, T. R., Teel, D. F., & Jacobs, R. J. (2008). Longitudinal chromatic aberration of the human infant eye. *Journal of the Optical Society of America, A, Optics, Image Science & Vision*, 25(9), 2263–2270.
- Whatham, A. R., & Judge, S. J. (2001). Compensatory changes in eye growth and refraction induced by daily wear of soft contact lenses in young marmosets. *Vision Research*, 41(3), 267–273.
- Wildsoet, C. F. (1997). Active emmetropization—evidence for its existence and ramifications for clinical practice. *Ophthalmic & Physiological Optics*, 17(4), 279–290.
- Wildsoet, C., & Wallman, J. (1995). Choroidal and scleral mechanisms of compensation for spectacle lenses in chicks. *Vision Research*, 35(9), 1175–1194.
- Zhou, X., Shen, M., Xie, J., Wang, J., Jiang, L., Pan, M., et al. (2008). The development of the refractive status and ocular growth in C57BL/6 mice. *Investigative Ophthalmology & Visual Science*, 49(12), 5208–5214.